

Received May 3, 2018, accepted June 15, 2018, date of publication July 4, 2018, date of current version September 21, 2018.

Digital Object Identifier 10.1109/ACCESS.2018.2850808

Frequency Selective Surface-Based Switched-Beamforming Antenna

GHADA HUSSAIN ELZWAWI^{ID}, HIFA HOUSSEIN ELZUWAWI, MUHAMMAD M. TAHSEEN, AND TAYEB A. DENIDNI, (Senior Member, IEEE)

Institut National de la Recherche Scientifique, University of Quebec, Montreal, QC H5A1K6, Canada

Corresponding author: Ghada Hussain Elzwawi (ghada.elzwawi@emt.inrs.ca)

This work was supported by the National Science and Engineering Research Council of Canada.

ABSTRACT A novel switched-beamforming antenna designed using active frequency selective surfaces (AFSS) is presented. The antenna consists of two parts: a source with an omnidirectional radiation pattern and a novel active triangular frequency selective surface (ATFSS) surrounding the source. Each unit cell in the ATFSS structure contains two diamond shaped patches connected with each other by a high-frequency pin-diode. The ATFSS elements are designed using CST microwave studio. The pin-diodes are applied to achieve beam switching. By switching the applied biasing voltage, the ON and OFF states of the ATFSS exhibit reflection and transmission characteristics in the operating WLAN band. By arranging the AFSS unit cells in a triangular structure with three panels and choosing different combinations of the diode states, the beam switching at various azimuthal directions is achieved. To validate this concept, the proposed antenna is fabricated and measured. A good agreement between simulations and measurements in terms of beam directions, reflection coefficient, and gain has been achieved @5.8 GHz.

INDEX TERMS Active frequency selective surface, directional radiation pattern, frequency selective surface, omnidirectional radiation pattern, switched-beamforming antenna, pin diode.

I. INTRODUCTION

The reconfigurable antenna is often characterized by its ability to adapt its behavior with changing system requirements and to provide additional levels of functionality for wireless communications. By using a reconfigurable antenna, the overall system performance can get rid of the restrictions that arise from the fixed characteristics of the conventional antennas [1]. The reconfigurable antenna concept based on determining the direction of arrival (DOA) of the incoming waves was introduced in [2] and [3]. Achieving multiple reconfigurable beams by using parabolic reflectors for satellite communication has been discussed in [4]. There are various techniques that can be used to steer the radiation pattern beam, such as integrated lens antennas (ILAs) [5], [6], traveling-wave antennas [7], [8], adaptive arrays [9], phased arrays [10], and active metallic photonic bandgap (AMPBG) [11].

Each of these technologies has some advantages as well as some disadvantages. For example, traveling wave antennas used for beam steering, hold a large size. For phased antenna arrays, the amplitude and phase of each individual element must be controlled to steer the beam in a specific direction, which complicates the structure and increases the

fabrication cost. The AMPBG is a bulky structure and suffers from higher side-lobe levels (SLL) and cross polarization. To overcome the design complexity, larger size, and expensiveness of the above-mentioned techniques, AFSSs have recently been used for achieving beam steering capability. Due to partial reflection/transmission behavior of the frequency selective surface (FSS), the radiation can either be transmitted or reflected in a specific desired direction.

In [12] an electrical beam steerable antenna has been proposed using an AFSS. The AFSS structure is connected with varactor diodes. By controlling the bias voltage, a 360° radiation pattern sweep is achieved for a single-beam mode and also for dual-beam modes. In spite of nonlinear behavior of the pin-diodes, these are most common components used to reconfigure the electromagnetic (EM) response of an FSS texture. The transmission/reflection characteristics of the pin-diodes, allow AFSS to control the direction of the incident EM waves [13]–[15]. For instance, in [13], 48 pin-diodes have been used in AFSSs to achieve beam-steering. This large number of active elements in the AFSS increases the complexity of the design as well as results higher fabrication cost. An AFSS-based beam-steering antenna with less number of active elements inserted in a cylindrical geometry has been

proposed in [15], where the antenna can sweep the entire azimuth plane with 60° radiation beamwidth in six steps, operating at 2.45 GHz.

This paper presents a new switched beamforming antenna using a novel ATFSS. The antenna comprises multiple AFSS, arranged in an equilateral triangle with three panels, and a feed placed in the middle of the structure used to excite the ATFSS. By applying multiple combinations of the diodes (ON and OFF) on each ATFSS panel, the beam-steering is achieved in various directions. The proposed beam-steering antenna can steer the beam in different directions in the azimuth plane with 120° radiation beamwidth. The proposed switched beamforming antenna provides a maximum realized gain of 7 dBi, which is almost 4 dBi higher than the feed gain. The antenna is fabricated and measured. The obtained results show a good agreement between simulations and measurements in terms of reflection coefficient, beam direction, and realized gain at 5.8 GHz.

The proposed antenna can be used in the upper WLAN WI-FI band (at 5.8 GHz), fixed satellites, radiolocation, first-person view (FPV), and other similar applications.

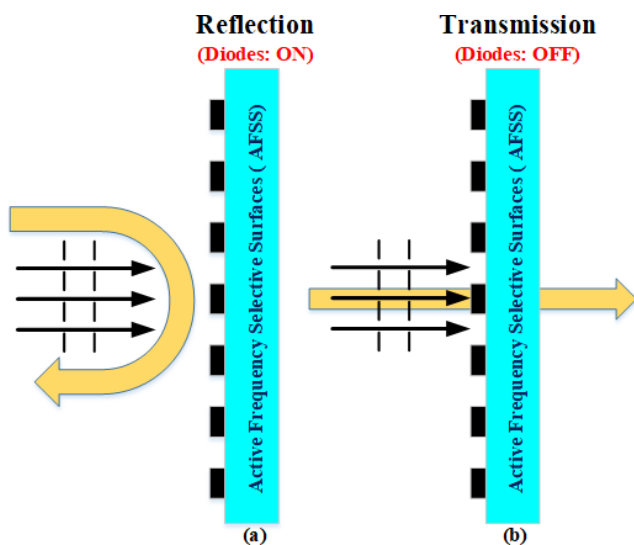


FIGURE 1. Basic principle of the AFSS in two diode states: (a) reflection, (b) transmission.

II. SWITCHED-BEAMFORMING ANTENNA DESIGN

The basic principle for an AFSS is shown in Fig. 1, where the surface can control the wave propagation by changing the features of the active components embedded in the FSS. By switching the diode's ON/OFF states, the reflection characteristic of the incident wave is achieved. The AFSS exhibits maximum reflection in the diode's ON state while maximum transmission in OFF state.

The proposed antenna consists of two main parts: first part comprises of three ATFSS panels arranged in an equilateral triangular configuration, while the second part is a patch with monopole radiation pattern used as a feed and placed in the middle of the structure.

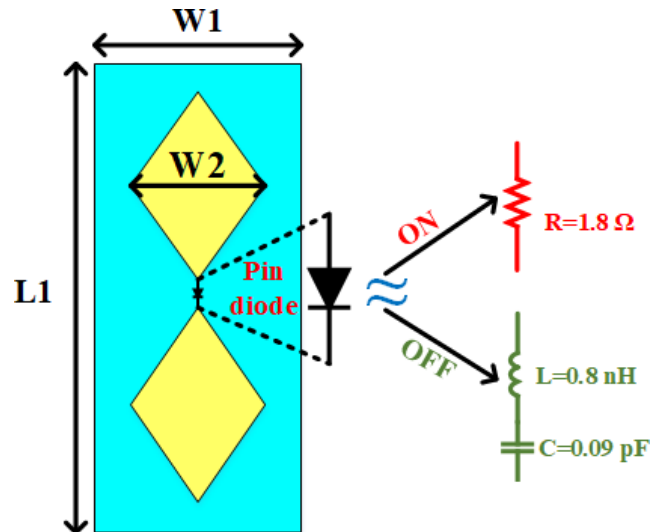


FIGURE 2. The proposed AFSS element with an equivalent circuit model of the diode's ON/OFF states.

A. ATFSS ELEMENT DESIGN

Each panel in the proposed AFSS consists of two unit cells as shown in Fig. 2. Each unit cell is subjected to either transmit or reflect the incoming waves in diode's ON or OFF state. To achieve this objective, an ATFSS element has been designed using CST Microwave Studio considering an infinite number of elements exist along the X- and Y-direction. Each element consists of two diamond shaped patches, which are electrically connected /disconnected from each other by the pin-diode.

The high-frequency pin-diode (GMP4202-GM1) is modeled as a series RLC circuit. A small resistance of $R_s = 1.8 \Omega$ represents the diode's forward bias (state ON), while a series capacitance of $C_p = 0.09 \text{ pF}$ and inductance of $L_p = 0.5 \text{ nH}$ exhibit the OFF state, as illustrated in the equivalent circuits shown in Fig. 2 [14]. A Y-polarized plane wave incidence is used to obtain the scattering characteristics from the element. The element is designed on Roger's RT/Duroid 5880 substrate with a thickness of 0.127 mm, a permittivity of 2.2, and loss tangent of 0.0009.

TABLE 1. The proposed ATFSS element dimensions.

Parameter	L1	W1	W2
Value (mm)	24	11	10

The effect of dielectric permittivity and substrate thickness on the scattering performance of the element in the ON/OFF states of the diode has been analyzed, as shown in Figs. 3(a) to (e). From this analysis, it is visible that dielectric permittivity as well as the thickness results in shifting the resonant frequency of the element. The dimensions of the ATFSS unit cell are summarized in Table 1. The results show that in the forward bias (ON state) the element exhibits maximum reflection, while in the OFF state depicts transmitting

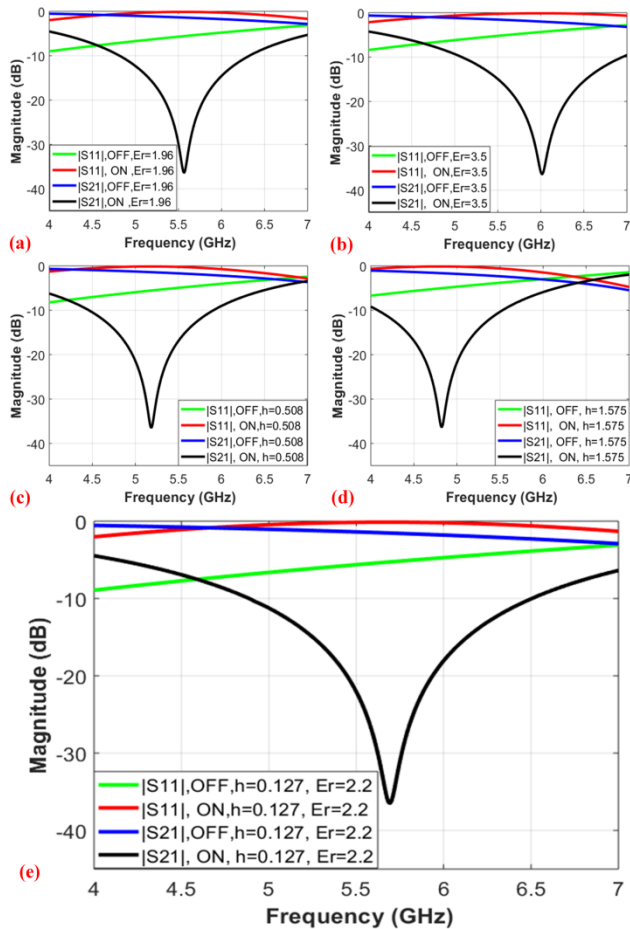


FIGURE 3. Scattering characteristics of the proposed unit cell in diode's ON/OFF states: (a), (b) The effect of dielectric permittivity, (c), (d) The impact of the substrate thickness, and (e) reflection and transmission coefficients of the proposed element.

characteristics at the operating frequency of 5.8 GHz. It has been observed that the proposed element exhibits a -5 dB difference in magnitude of the reflected wave, while a -21 dB magnitude difference in the transmitted wave in both diode's ON and OFF states (at 5.8 GHz).

Effect of the element size as well as the size of radiating patches on the scattering performance have also been analyzed. Fig. 4, depicts that when the element size 'W1' is increased, the resonance frequency shifts to lower frequency band. The effect of radiating patch size 'W2' on the scattering performance is shown in Fig. 5, which shows that change in the size of the diamond-shaped patch also shifts the resonant frequency. These parameters were optimized to operate in the desired frequency band.

For deeper investigation, a near field analysis at the AFSS is performed. Fig. 6 (a), (b) illustrate the magnitude of electric field distribution on the proposed AFSS element at $Z = 0$ plane at 5.8 GHz. It is evident that the intensity of electric field magnitude is maximum in ON state (reflection) while it is minimum in the diode's OFF state (transmission). The highest field strength of 4500 V/m is observed at the radiating edges at the center as well as at the vertical edges near the

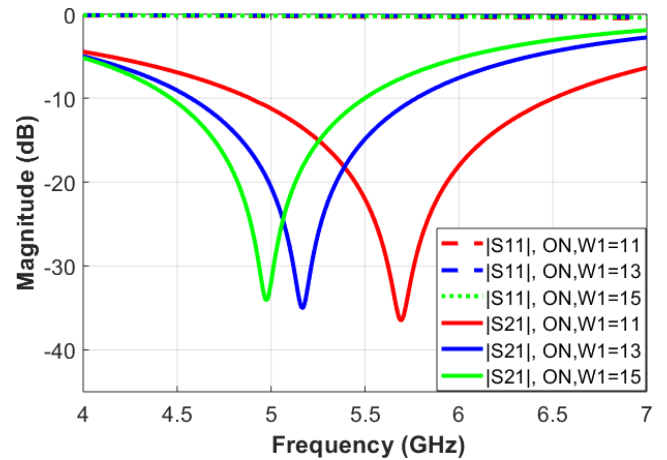


FIGURE 4. Effect of element size on the scattering performance in diode's ON states.

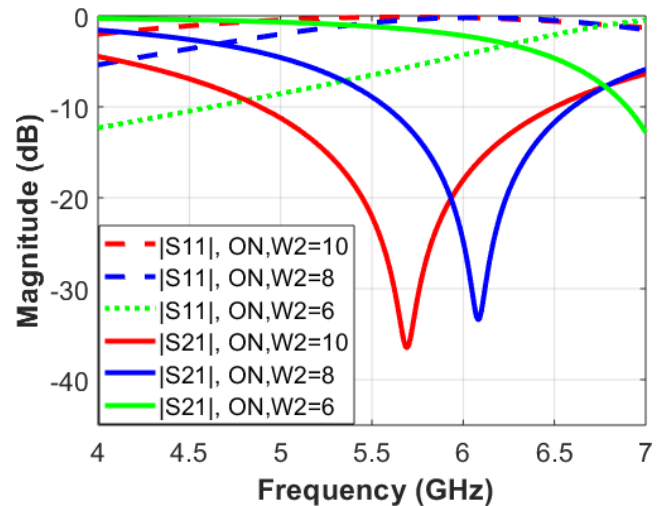


FIGURE 5. Effect of radiating patch size on the scattering performance in diode's ON states.

cell boundary. This higher field strength near the cell boundary is mainly due to coupling between adjacent elements. The minimum field intensity is observed in most central part of the element in diode's OFF state, which allows the incident waves to transmit to the other side.

B. FEED DESIGN

To excite the AFSS elements from all directions, an antenna with monopole radiation pattern is required. To achieve this objective, a rectangular patch antenna, shown in Fig. 7, is designed on Rogers RO-3006 substrate with a relative dielectric permittivity of 6.15, thickness of 1.27 mm, and a loss tangent of 0.002. The feed parameters are optimized to provide a better antenna performance in the operating band, as well as achieving compactness for minimum blockage. Table 2 shows the optimized parameters of this monopole antenna. The feed has the size of 18 mm \times 10 mm. The feed is fabricated and measured, as shown in Fig. 7 (b). The simulated and measured reflection coefficient and

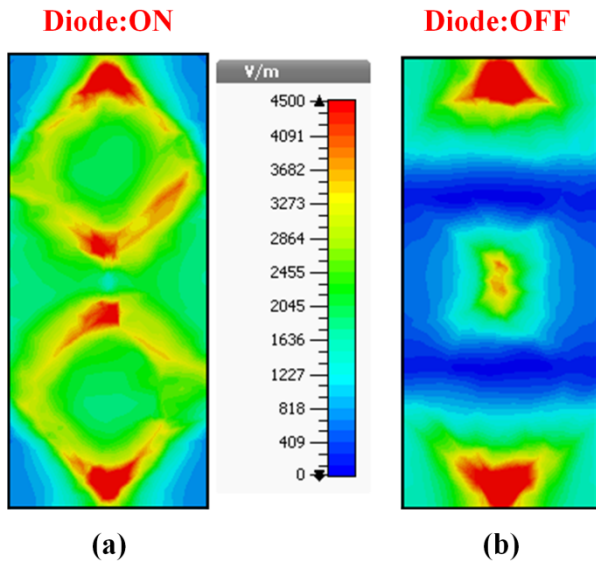


FIGURE 6. Near field analysis on the proposed AFSS element surface: reflection state. (b) transmission state.

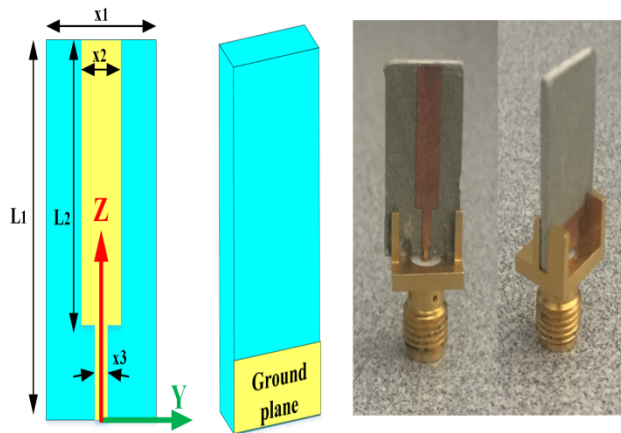


FIGURE 7. Simulated and fabricated feed antenna model to excite ATFSS elements.

TABLE 2. The feed dimensions.

Parameter	L1	L2	L3	x1	x2	x3
Value(mm)	18	13.15	3.5	10	3.0	1.2

radiation pattern show reasonably good agreement, as shown in Fig. 8, and Fig. 9, respectively.

C. SWITCHED BEAMFORMING ANTENNA DESIGN

The operational mechanism of the proposed switched beamforming antenna is based on converting the omnidirectional radiation pattern of the source into the directional one by using the proposed ATFSS. When the pin-diodes of ATFSS are switched OFF, the ATFSS behaves like a transmitting surface, while in the ON state, it acts as a reflecting surface. The ATFSS screens are arranged in an equilateral triangle to switch the beam in multiple directions using different combinations of the ATFSS diodes. Fig. 10 shows the top and side 3-D view of the proposed antenna. In this design,

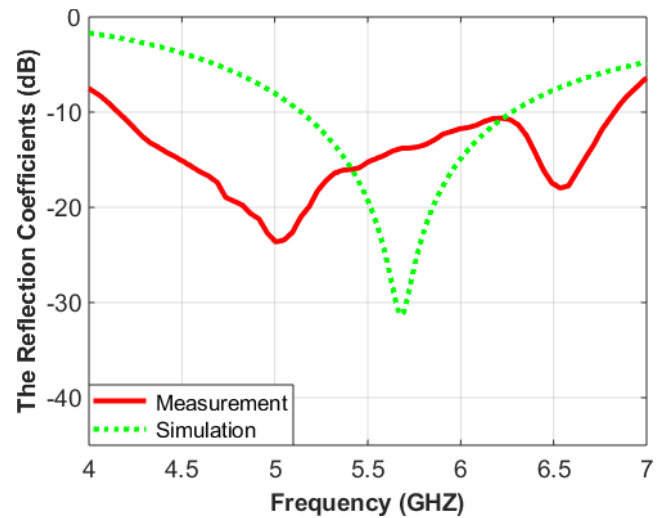


FIGURE 8. Simulated and measured reflection coefficient of the feed.

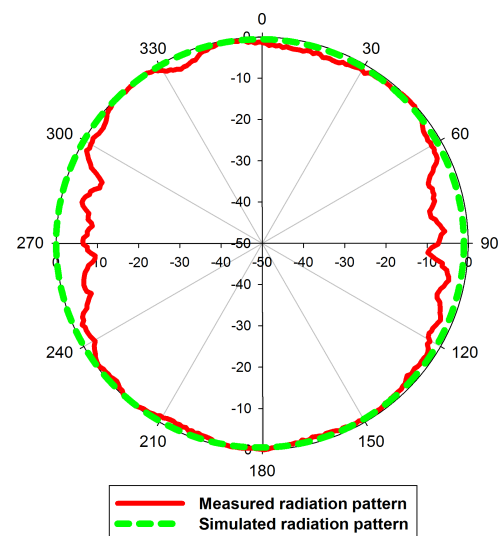


FIGURE 9. Simulated and measured radiation patterns in the H plane of the monopole patch antenna.

each step sweeps the beam 120° in the azimuth direction. The schematic diagrams illustrating the operating mechanism of the proposed antenna and the simulated results of three beam steering steps (different combinations) are shown in Fig. 11 (a), (b).

The effect of feed position offset ‘d1’ on the performance of the proposed antenna in terms of reflection coefficient, realized gain, and the radiation pattern has also been investigated, and results are presented in Fig. 12 to Fig. 14. The presented results exhibit that as the feed moves away from the central position (for example, away from Side 3 towards positive X-axis), the resonant frequency shifts towards the upper band. This shift in the resonant frequency also effects on reducing the realized gain, as well as narrows the half power beamwidth (HPBW) of the antenna. It is also evident that the feed position of $d1 = 4$ mm gives the best antenna performance, justifying the selection of this distance.

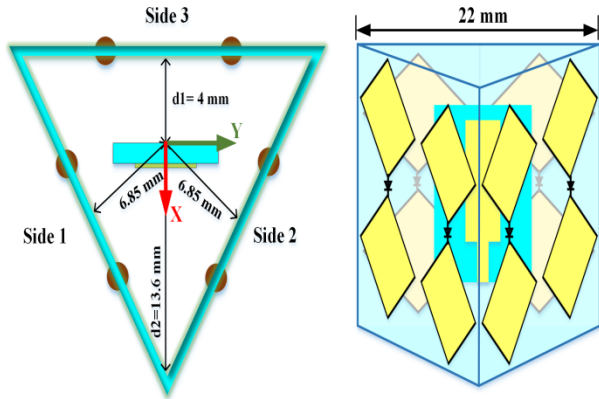


FIGURE 10. Simulated model of the proposed ATFSS antenna in, top and side 3-D view.

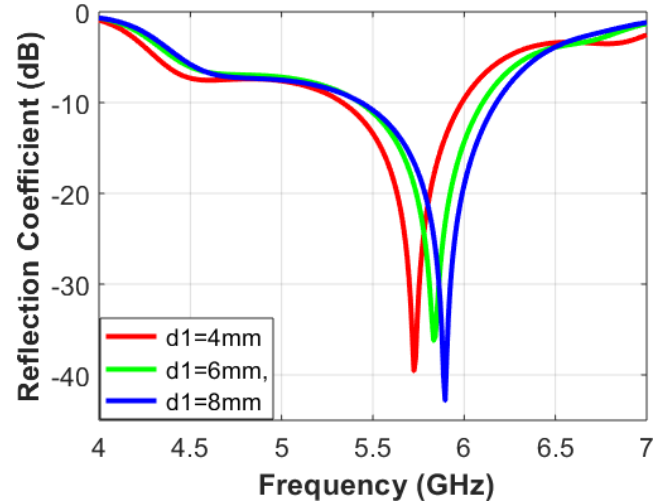


FIGURE 12. Effect of feed offset 'd1' in 'Combination C' on the simulated reflection coefficient.

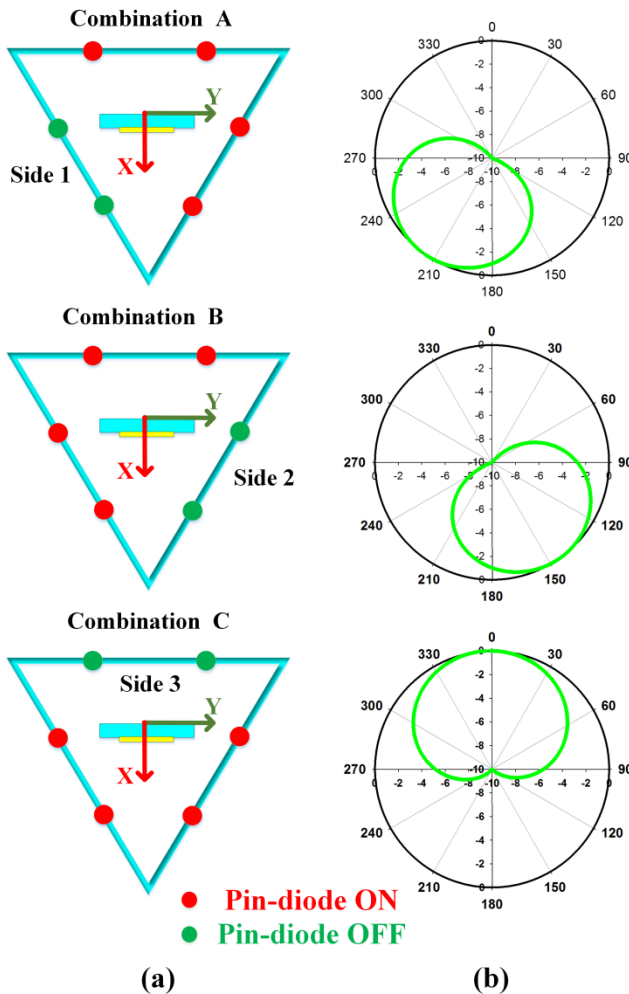


FIGURE 11. Sketch of the proposed ATFSS antenna, (a) with multiple combinations of the diodes for steering the beam in various directions, and (b) the simulation results in each combination.

D. SWITCHED BEAMFORMING ANTENNA DESIGN USING DIPOLE AS A SOURCE

To evaluate the effect of feeding source on the proposed antenna performance, the patch antenna is replaced by a dipole as shown in Fig. 15. The same previous three

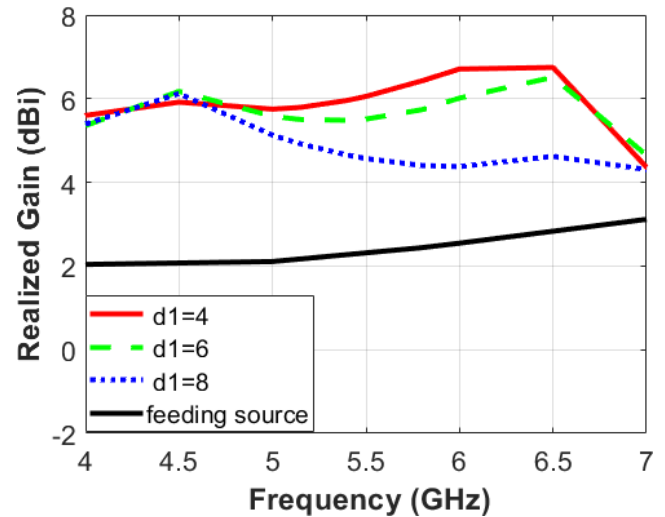


FIGURE 13. Effect of feed offset 'd1' in 'Combination C' on the simulated realized gain.

combinations of the diodes shown in Fig. 11, are re-applied on the proposed ATFSS antenna. The simulated reflection coefficient, gain and radiation patterns of the proposed antenna using dipole source for different diode states are shown in Fig. 16 to Fig. 18. The comparison of the proposed antenna gain using two different feed sources is summarized in Table 3 and Table 4. Based on the compared results, it is visible that both feeds result almost similar performance. However, the patch antenna with monopole radiation pattern is selected for fabrication and measurements due to its ease in fabrication and better handling during measurements.

III. FABRICATION AND MEASUREMENT RESULTS

The proposed switched beamforming antenna is fabricated and measured. Fig. 19, shows multiple steps applied to assemble the fabricated antenna, and the measurement setup.

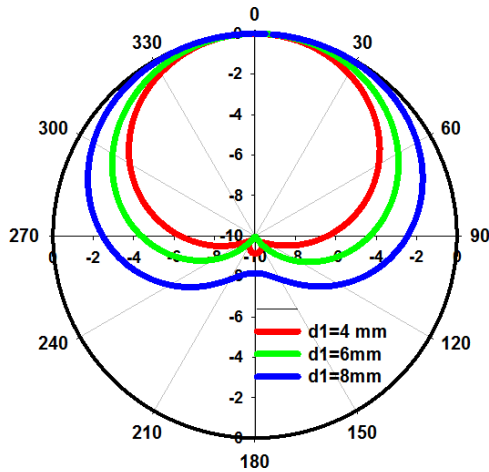


FIGURE 14. Effect of feed offset 'd1' in 'Combination C' on the simulated radiation patterns in H-plane.

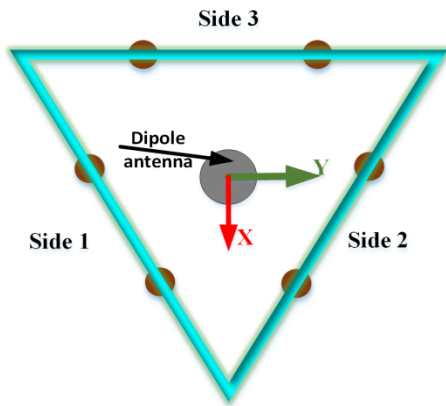


FIGURE 15. Top view of the proposed active triangular FSS antenna using dipole as a source of EM waves.

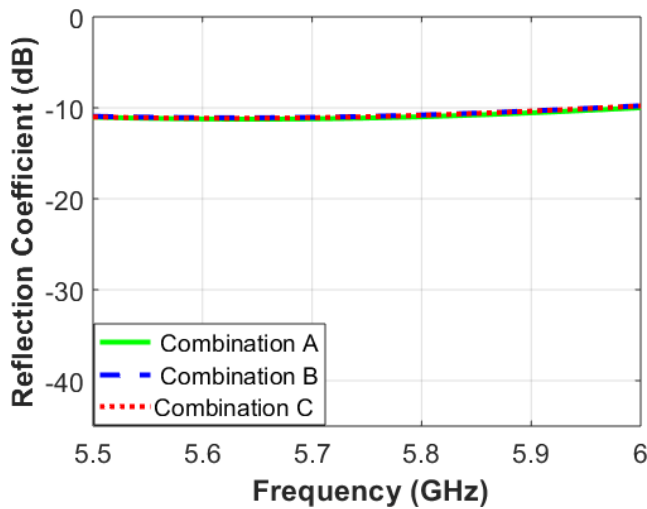


FIGURE 16. Simulated reflection coefficient of the proposed ATFSS antenna.

In Step 1, an array of 2×6 passive FSS elements is fabricated. In Step 2, the unit cells are wrapped onto equilateral triangular foam to form AFSS. Due to the minimum

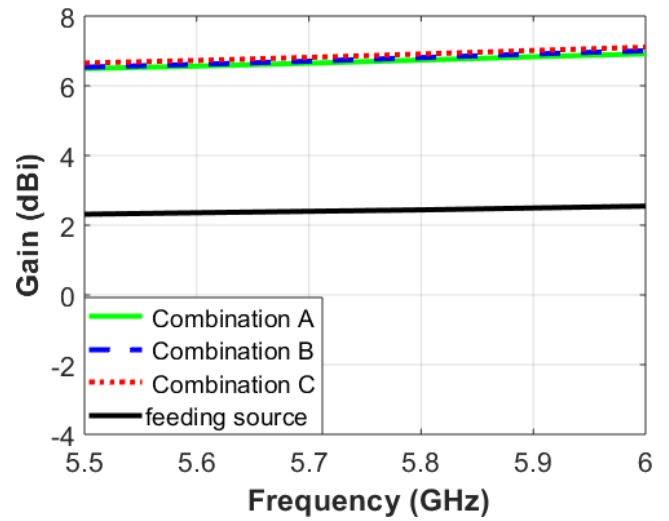


FIGURE 17. Simulated gain of the proposed ATFSS antenna.

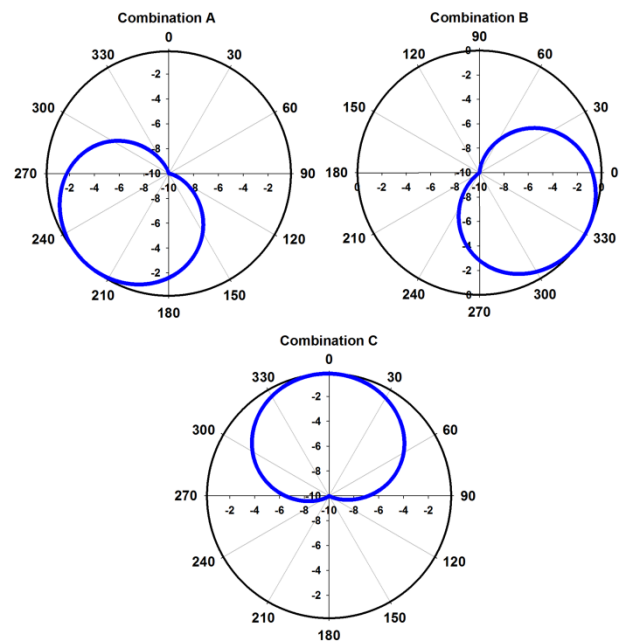


FIGURE 18. Simulated radiation pattern of the proposed switched beamforming ATFSS antenna with dipole feed (in combination C).

TABLE 3. Simulated Gain Comparison in three used combinations along with the dipole used as a source (at 5.8 GHz).

Combination	Gain (dBi)
Comb. A	6.7364
Comb. B	6.8074
Comb. C	6.9122
Dipole	2.1870

dielectric thickness, the wrapping is done with ease but for an array designed on a material with larger substrate thickness can be arranged by cutting each side separately and binding

TABLE 4. Gain Comparison in three used combinations along with the Patch used as a source (at 5.8 GHz).

Combination	Gain (dBi)
Comb. A, sim.	6.264
Comb. A, meas.	5.437
Comb. B, sim.	6.280
Comb. B, meas.	5.394
Comb. C, sim.	6.289
Comb. C, meas.	5.816
Patch sim.	2.439
Patch meas.	2.236

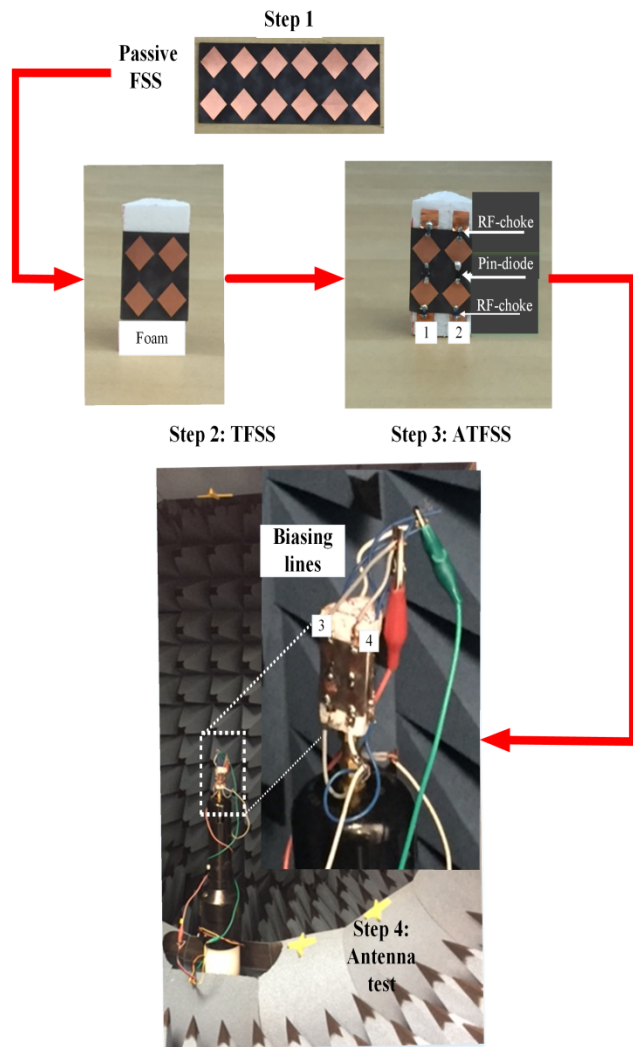


FIGURE 19. Prototyping steps and measurement picture of the fabricated ATFSS antenna in an anechoic chamber.

their corner junctions using either glue or smallest diameter available plastic screws. While in Step 3, a high-frequency pin-diode is soldered in each passive FSS unit cell to form ATFSS element. To isolate the RF signal from DC biasing lines, RF chokes are used at top and bottom sides of each element. All the connections required a positive DC voltage

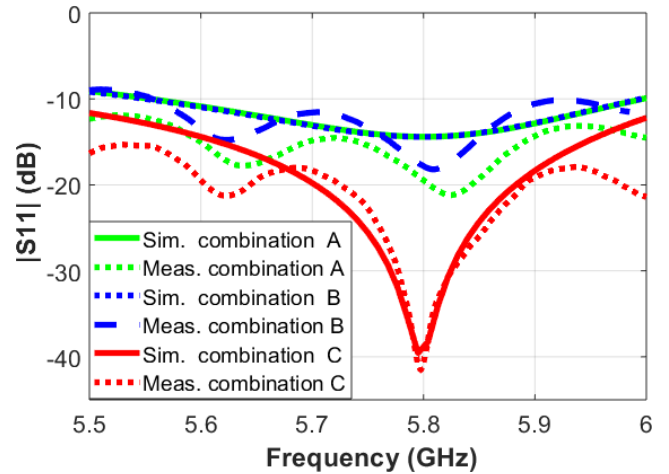


FIGURE 20. Simulated and measured reflection coefficient of the proposed switched beamforming ATFSS antenna.

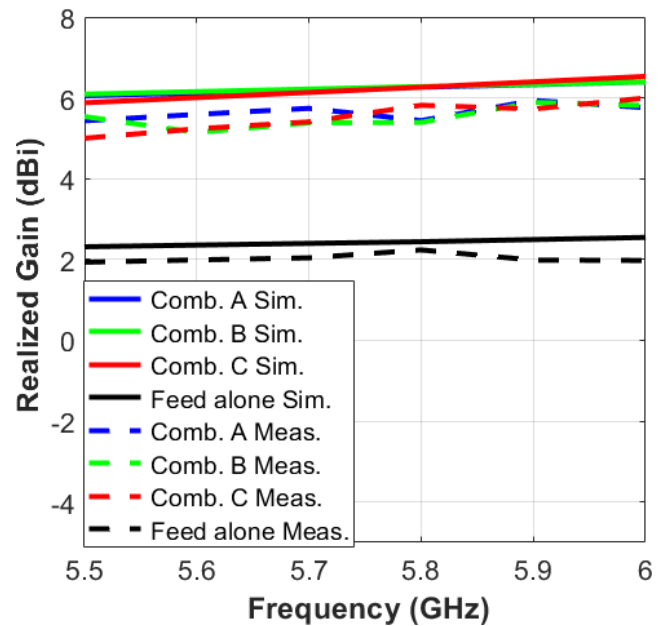


FIGURE 21. Simulated and measured gain of the proposed switched beamforming ATFSS antenna.

supply are connected in parallel to make a single node, while all the GND connections are also unified making the second node (at the bottom). When the DC supply voltage of 1.2 V is applied, the diodes in AFSS operate in ON state, while 0V represents the OFF state. The antenna radiation pattern is measured in the anechoic chamber.

The simulated and measured reflection coefficient, gain and radiation patterns of the proposed antenna in the azimuth plane ($\theta = 90^\circ$) for different diode states are shown in Fig. 20 to Fig. 22. It is visible that the omnidirectional radiation pattern of the source antenna is converted into a directional pattern by using the proposed ATFSS switched beamforming screens. When the diodes in side 1 are OFF (combination A), the pattern is directed toward 240° , when the diodes in side 2 are OFF (combination B), the pattern is

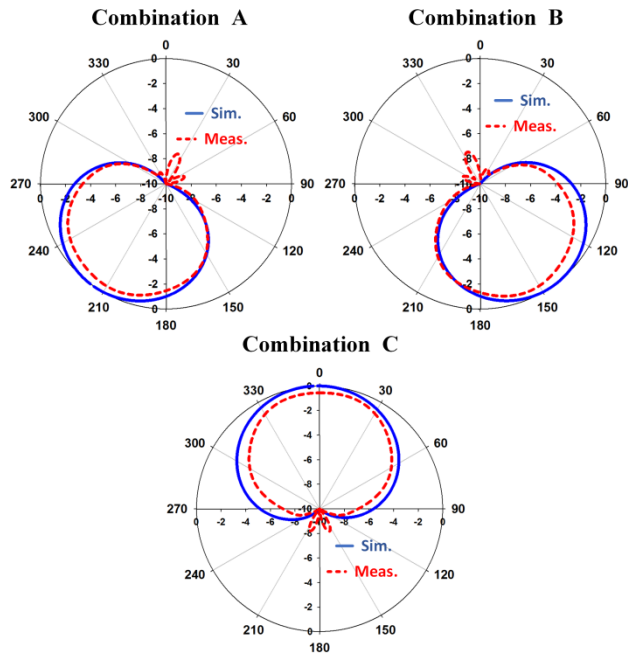


FIGURE 22. Simulated and measured radiation patterns of the proposed switched beamforming ATFSS antenna (in combination C).

directed towards 120° , and when the diodes in side 3 are OFF (combination C), the pattern is oriented toward 0° . Other beam steering directions can be achieved by choosing different sectors ON/OFF state combinations. With this feature, the proposed antenna provides beam steering flexibility in the azimuth plane. The simulation and measurements show reasonably good agreement.

IV. CONCLUSION

This paper has presented a new switched beamforming antenna using an active triangular frequency selective surface. The antenna consists of two parts: an FSS screen loaded with pin-diodes arranged in an equilateral triangle, and a radiating source with omnidirectional radiation pattern placed at the center of the structure. By applying multiple combinations of the diodes (in ON and OFF states) on each ATFSS screens, the switched beamforming has been achieved in various directions. The proposed switched beamforming antenna has shown the ability to sweep the radiations in the azimuth plane using three pin diode combinations on the ATFSS. The antenna has been fabricated and measured. Simulations and measurements have shown good agreement, in terms of reflection coefficient, beam directions, and realized gain.

REFERENCES

- [1] J. Bernhard, *Reconfigurable Antennas*. San Rafael, CA, USA: Morgan & Claypool, 2007.
- [2] H. T. Friis, C. B. Feldman, and W. M. Sharpless, "The determination of the direction of arrival of short radio waves," *Proc. Inst. Radio Eng.*, vol. 22, no. 1, pp. 47–78, Jan. 1934.
- [3] E. W. Matthews, C. L. Cuccia, and M. D. Rubin, "Technology considerations for the use of multiple beam antenna systems in communication satellites," *IEEE Trans. Microw. Theory Techn.*, vol. MTT-27, no. 12, pp. 998–1004, Dec. 1979.

- [4] A. Hakkarainen *et al.*, "Reconfigurable antenna based doa estimation and localization in cognitive radios: Low complexity algorithms and practical measurements," in *Proc. CROWCOM*, Oulu, Finland, Jun. 2014, pp. 454–459.
- [5] A. Mozharovskiy, A. Artemenko, A. Sevastyanov, V. Ssorin, and R. Maslennikov, "Beam-steerable integrated lens antenna with waveguide feeding system for 71–76/81–86 GHz point-to-point applications," in *Proc. EuCAP*, Davos, Switzerland, Apr. 2016, pp. 1–5.
- [6] A. Abbaspour-Tamijani, L. Zhang, G. Pan, H. K. Pan, and H. Alavi, "Lens-enhanced phased array antenna system for high directivity beam-steering," in *Proc. APSURSI*, Spokane, WA, USA, Jul. 2011, pp. 3275–3278.
- [7] T. Ueda, S. Yamamoto, Y. Kado, and T. Itoh, "Pseudo-traveling-wave resonator with magnetically tunable phase gradient of fields and its applications to beam-steering antennas," *IEEE Trans. Microw. Theory Techn.*, vol. 60, no. 10, pp. 3043–3054, Oct. 2012.
- [8] Y. Yokohama and T. Kodera, "Voltage beam-steerable leaky-wave antenna using magnet-less non-reciprocal metamaterial (MNM)," in *Proc. ISAP*, Hobart, TAS, Australia, Nov. 2015, pp. 1–3.
- [9] T. A. Denidni and G. Y. Delisle, "A nonlinear algorithm for output power maximization of an indoor adaptive phased array," *IEEE Trans. Electromagn. Compat.*, vol. 37, no. 2, pp. 201–209, May 1995.
- [10] V. S. Rao, V. V. Srinivasan, and S. Pal, "Generation of dual beams from spherical phased array antenna," *Electron. Lett.*, vol. 45, no. 9, pp. 441–442, Apr. 2009.
- [11] G. Poilasne, P. Pouliguen, K. Mahdjoubi, L. Desclos, and C. Terret, "Active metallic photonic band-gap materials (MPBG): Experimental results on beam shaper," *IEEE Trans. Antennas Propag.*, vol. 48, no. 1, pp. 117–119, Jan. 2000.
- [12] L. Zhang, Q. Wu, and T. A. Denidni, "Electronically radiation pattern steerable antennas using active frequency selective surfaces," *IEEE Trans. Antennas Propag.*, vol. 61, no. 12, pp. 6000–6007, Dec. 2013.
- [13] A. Edalati and T. A. Denidni, "High-gain reconfigurable sectoral antenna using an active cylindrical FSS structure," *IEEE Trans. Antennas Propag.*, vol. 59, no. 7, pp. 2464–2472, Jul. 2011.
- [14] J. Li, T. A. Denidni, and Q. Zeng, "Beam switching antenna based on active frequency selective surfaces," in *Proc. IEEE NEMO*, Ottawa, ON, Canada, Aug. 2015, pp. 1–3.
- [15] J. Li, T. A. Denidni, and Q. Zeng, "A dual-band reconfigurable radiation pattern antenna based on active frequency selective surfaces," in *Proc. APSURSI*, Fajardo, Puerto Rico, Jun./Jul. 2016, pp. 1245–1246.



GHADA HUSSAIN ELZWAWI received the B.Sc. degree in electrical and electronics engineering from the Faculty of Engineering, University of Benghazi, Libya, in 2003, and the M.Sc. degree in electrical and electronics engineering (telecommunications) from Benghazi University in 2009. From 2004 to 2006, she was an Engineer with Libya Mobile Phone Company, Benghazi, Libya. From 2007 to 2014, she was a Lecturer with the Technical College of Mechanical Engineering, Benghazi.

She is currently pursuing the Ph.D. degree in telecommunications from the Energy, Materials and Telecommunications Center, Institut National de la Recherche Scientifique, University of Quebec, Montreal, QC, Canada.

Her current research interests include reconfigurable antennas, frequency selective surfaces, and reconfigurable reflectarray.



HIFA HOUSSEIN ELZWAWI received the B.Sc. degree in electrical and electronics engineering from Garyounis University, Benghazi, Libya, in 2000.

She is currently pursuing the M.Sc. degree in telecommunications with the Energy, Materials and Telecommunications Center, Institut National de la Recherche Scientifique, University of Quebec, Montreal, QC, Canada. From 2001 to 2014, she was an Instructor with the Engineering Department, College of Electrical and Electronics Technology, Benghazi.



MUHAMMAD M. TAHSEEN received the B.Sc. degree in electrical engineering and telecommunications from the COMSATS Institute of Information Technology, Lahore, Pakistan, in 2008, the M.Sc. degree in electrical engineering and radio communications from the Blekinge Institute of Technology, Karlskrona, Sweden, in 2011, and the Ph.D. degree in electrical and computer engineering from Concordia University, Montreal, QC, Canada, in 2017.

Dr. Tahseen is currently a Post-Doctoral Fellow in a collaborative research project between Concordia University, and INRS-EMT, Montreal. In 2008, he was with the Network Management Center, Pakistan, Telecommunication Company Limited, Lahore. From 2012 to 2017, he was a Teaching and Research Assistant with Concordia University.

Dr. Tahseen was a recipient of the Concordia University Cross-Department Research Fellowship “FOYER”. His paper was honored with the Best Student Paper Award in ANTEM 2016.

He is an IEEE reviewer for several journals and conferences: TRANSACTIONS ON ANTENNAS AND PROPAGATION, *IET Electronics Letters*, and PIER.

His current research interests include reconfigurable antennas, wearable antennas, parabolic reflectors, reconfigurable reflectarrays, and lens and frequency selective surfaces.



TAYEB A. DENIDNI (SM'04) received M.Sc. and Ph.D. degrees in electrical engineering from Laval University, Quebec, QC, Canada, in 1990 and 1994, respectively.

From 1994 to 2000, he was a Professor with the Engineering Department, University of Quebec in Rimouski, Rimouski, QC, Canada, where he founded the Telecommunications Laboratory.

Since 2000, he has been with the Institut National de la Recherche Scientifique (INRS), University of Quebec, Montreal, QC, Canada. He found the RF laboratory at INRS-EMT, Montreal. He has a great experience with antenna design and he is leading a large research group consisting of three research scientists, six Ph.D. students, and one M.Sc. student. His current research areas of interest include reconfigurable antennas using EBG and FSS structures, dielectric resonator antennas, metamaterial antennas, adaptive arrays, switched multi-beam antenna arrays, ultra-wideband antennas, and microwave and development for wireless communications systems. In 2012 and 2013, he was awarded by INRS for outstanding research and teaching achievements and an investigator on many research project sponsored by NSERC, FCI and numerous industries. He served as a principal Editor for the *IET Electronics Letters*.

Since 2015, he has been served as an Associate Editor for the *IET Electronics Letters*. From 2005 to 2007, he has served as an Associate Editor for the IEEE ANTENNAS WIRELESS PROPAGATION LETTERS. From 2008 to 2010, he served as an Associate Editor for the IEEE TRANSACTIONS ON ANTENNAS PROPAGATION.

• • •